The Quasi-Hydrostatic Approximation

ISIDORO ORLANSKI

Geophysical Fluid Dynamics Laboratory/NOAA, Princeton University, Princeton, NJ 08540

(Manuscript received 17 June 1980, in final form 24 November 1980)

ABSTRACT

Second-order expansion of the aspect ratio gives rise to simple equations with a quasi-hydrostatic approximation that perform far better than the classical hydrostatic system in the simulation of moist convection in a mesoscale model. It also suggests that a simple modification to this system may extend the validity of schemes for aspect ratios larger than 1.

1. Introduction

One of the prominent features of large circulations in most geophysical systems is the balance between the vertical pressure gradient and its weight.

For the hydrostatic balance to be valid, a simple scale analysis can prove that the ratio of the vertical scale to the horizontal scale H/L must be much smaller than 1. In this flow regime, the particle motion of the fluid will be in horizontal planes with only the static balance of the forces acting in the vertical. Then it follows that for fluid motion where horizontal scales are comparable to the vertical scales, the vertical acceleration of the particles can no longer be assumed smaller than the vertical pressure gradients and the hydrostatic assumption breaks down. The hydrostatic balance assumption greatly simpifies the procedure to solve the equations of motion. Accordingly, this was extensively used in theoretical work on large scale circulation of the atmosphere and the oceans. Certainly, the area which benefited most from this simplification was the work related to numerical modeling of such phenomena. The simplification for numerical modeling lies not only in the elimination of the vertical momentum equation, which certainly is a considerable reduction. By assuming hydrostatic balance, the compressible equation with explicit sound waves need not be solved in the vertical, thus permitting a much larger integration time step and hence a shorter model run time. The benefits of the hydrostatic balance are further appreciated if the anelastic equations (sound free) are used, in which a three-dimensional Poisson equation needs to be solved to retrieve the pressure field and thus causing an even more expensive integration. These limitations of integration with the complete equations may have been part of the reason why cloud modeling (non-hydrostatic) is lagging behind global circulation modeling (hydrostatic). Comparable hydrostatic and non-hydrostatic models may have a ratio of one to ten for the time it takes to integrate each model.

The rapid technological development of meteorological instruments in recent years has made continuous observation of mesoscale phenomena possible. Limitations to numerical simulation of mesoscale processes have not only been due to incompleteness of past observational data but also to unavailability of appropriate mesoscale models. The strict adaptation of GCM's was realized not to be the correct one because the hydrostatic assumption built into such models is the limiting factor for its use in simulating the mesoscales. On the other hand, upgrading of cloud dynamics models, which should cover a horizontal extension for mesoscale phenomena to be well resolved, becomes overwhelmingly expensive.

It seems clear from the previous discussion that a practical approach to encompass the limitations of hydrostatic models is to find an appropriate extension of the hydrostatic balance that will be well behaved to the limits of the mesoscale range. The purpose of this paper is to present such an extension, the quasi-hydrostatic approximation, which has these characteristics.

2. Higher order expansion in the aspect ratio (H/L)

The small aspect ratio between the vertical and horizontal scales of motion is the well-known justification necessary for the hydrostatic balance to be valid. However, to describe why the assumption is violated when the aspect ratio is of the order of one is not so trivial. Let us then look at the simple dispersion relation for internal gravity waves in a stratified rotating fluid at rest.

a. The dispersion relation

The frequency ω for the waves is given by

$$\omega = \pm\left[\frac{(k^2 + l^2)N^2 + \gamma^2 f^2}{k^2 + l^2 + \gamma^2}\right]^{1/2}, \quad (2.1)$$

where k, l and γ are the horizontal x, y and vertical z wavenumbers, respectively; and N and f are the Brunt-Väisälä frequency (assumed constant) and the Coriolis parameter, respectively. In nondimensional form

$$\omega = \pm\left[\frac{(K^2 + L^2)N^2\delta^2 + p^2 f^2}{[\delta^2(K^2 + L^2) + p^2]}\right]^{1/2}, \quad (2.2)$$

where $\delta = H/L$ is the aspect ratio. In the hydrostatic limit $\delta \ll 1$

$$\omega_H = \pm[(K^2 + L^2)\delta^2 N^2 + p^2 f^2]^{1/2} P^{-1}. \quad (2.3)$$

The large value of N compared with f for atmospheric conditions ($N \approx 10^{-2}$ s^{-1}; $f \approx 10^{-4}$; $\delta \approx 10^{-2}$) leaves the numerator unchanged and only the vertical wavenumber p represents the total wavenumber in the denominator. Trajectory particles are close to being horizontal. For larger $\delta \approx 10^{-1}$ the stratification is the dominant term in the numerator

$$\omega_H = \pm[(K^2 + L^2)\delta^2 N^2]^{1/2} P^{-1}. \quad (2.4)$$

In fact, the hydrostatic assumption basically neglects the horizontal wavenumbers in comparison with the vertical wavenumbers and this would not be a serious inconvenience since only the highest frequency waves in the hydrostatic system would be distorted. However, when the possibility of convective instability exists ($N^2 < 0$), Eq. (2.4) becomes

$$\omega_H = \pm i[(K^2 + L^2)\delta^2 N^2]^{1/2} P^{-1}. \quad (2.5)$$

So the larger the aspect ratio δ is, the larger the growth rate of the unstable waves will be. Inspecting the non-hydrostatic dispersion relation for this case (2.2), we find that

$$\omega_{NH} = \pm i\frac{[(K^2 + L^2)\delta^2 N^2]^{1/2}}{[(K^2 + L^2)\delta^2 + p^2]^{1/2}}. \quad (2.6)$$

For large $\delta \gg 1$, $\omega_H \propto \delta N$, whereas $\omega_{NH} \propto N$. The growth rate of convection, therefore, in a non-hydrostatic system will be bounded, whereas the hydrostatic system will not be. This process is even more enhanced for convection in a moist unstable atmosphere. For a δ even smaller than 1, the hydrostatic set of equations will become unrealistically unstable and more unstable for the higher horizontal wavenumbers. Since those waves are not well resolved by the model, the numerical integration deteriorates (Miyakoda and Rosati, 1977).

b. Expansion in the two-dimensional linear equations

We assume for simplicity that the motion is two dimensional. The linear equations for the stratified fluid are

$$\zeta_{t't'} + N^2\phi_{x'x'} = 0, \quad (2.7)$$

where ζ is the vorticity ($\zeta = \nabla^2\phi$) and ϕ, the streamfunction, may be written

$$(\phi_{x'x'} + \phi_{z'z'})_{t't'} + N^2\phi_{x'x'} = 0.$$

If nondimensional coordinates are defined as

$$X' = Lx; \quad Z' = Hz; \quad t' = Nt,$$

then

$$(\delta^2\phi_{xx} + \phi_{zz})_{tt} + \delta^2\phi_{xx} = 0. \quad (2.8)$$

Solutions of (2.8) are of the form $e^{i\omega t}$. We now expand ω and ϕ in order δ as

$$\left.\begin{aligned}\omega^2 &= \delta^2\omega_0^2 + \delta^4\omega_1^2 + \cdots\\ \phi &= \phi_0 + \delta^2\phi_1 + \cdots\end{aligned}\right\}. \quad (2.9)$$

Substituting the expansion (2.9) into (2.8) and separating by order of δ, it follows that to order $O(\delta^2)$

$$-\omega_0^2\phi_{0zz} + \phi_{0xx} = 0, \quad (2.10)$$

and to order $O(\delta^4)$

$$-\omega_0^2(\phi_{0xx} + \phi_{1zz}) - \omega_1^2\phi_{0zz} + \phi_{1xx} = 0 + \phi(\delta^6).$$

The order of δ^2 of (2.10) gives the hydrostatic dispersion relation $\omega_0^2 = K^2/p^2$ and to the $O(\delta^4)$ the correction to the streamfunction ϕ_1 cancelled because it has the same expression as (δ^2); the rest of (δ^4) gives the correction to the frequency squared

$$\omega_1^2 = -\omega_0^2 K^2/P^2.$$

To this second order, the dimensional frequency squared will be

$$\omega^2 = \frac{k^2}{\gamma^2}N^2\left(1 - \frac{k^2}{\gamma^2}\right). \quad (2.11)$$

This frequency is the same as that obtained by expanding (2.2) to higher orders $O(k/\gamma)^2$ which is equivalent to our previous analysis.

The equations derived by retaining the second term (δ^4) in the expansion of the aspect ratio we named the quasi-hydrostatic equations and the frequency as defined in (2.11) corresponds to the dispersion relation for internal gravity waves assuming the quasi-hydrostatic approximation ω_{QH}.

We now discuss the properties of ω_{QH} as compared to ω_H and ω_{NH}. Fig. 1 shows the square of the three frequencies as a function of $(k/\gamma)^2$. The behavior of all three frequencies is similar for (k/γ) very small; ω_{QH}^2 has a maximum at $(k/\gamma) = 0.7$. For this value of (k/γ), the frequencies are

$$\omega_H^2 = N^2/2, \quad \omega_{QH}^2 = N^2/4, \quad \omega_{NH}^2 = N^2/3.$$

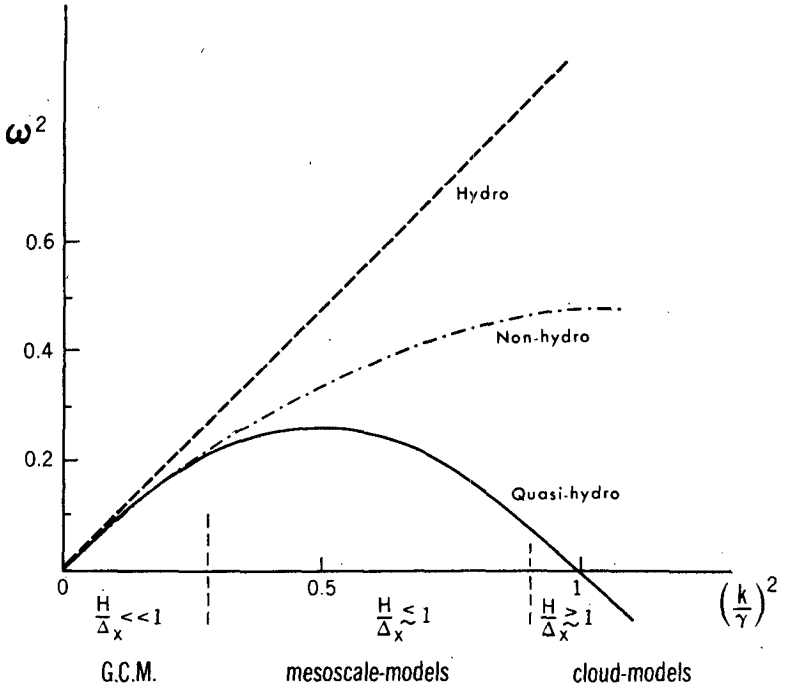

FIG. 1. The dispersion curves for different approximations. The validity of current numerical models is pointed out.

In spite of this rather large aspect ratio, the differences between the different approximations are not substantial. Differences between the approximations are shown for $k/\gamma \sim 1$ or $2H/\Delta x$ (Δx is the horizontal grid for the numerical model) the highest aspect ratio obtained in a numerical model. For such limits the hydrostatic system will be much more unstable than either the non-hydrostatic or the quasi-hydrostatic system. On the other hand, the latter scheme is much more stable for aspect ratios close to unity. In finite-difference models those waves are poorly resolved ($k \sim \pi/\Delta x$) and are regarded as noise.

The tremendous advantage of the quasi-hydrostatic system over the hydrostatic system can be viewed in the following way: when the systems are applied to unstable atmospheric disturbances where H/L is very small, the solution will be equally well resolved in either system unless nonlinear feedback from higher scales is important. In that case, for disturbances where $H/L \leq 1$, the quasi-hydrostatic system will probably better simulate those waves with scales larger than a few grid sizes. For grid size disturbances, however, neither of the two systems will be able to produce an acceptable simulation. Additionally, because truncation errors limit its resolution, the quasi-hydrostatic system has the ability to restrain the unrealistic growth of such errors which inherently will grow in the hydrostatic system. [Large amounts of rainfall were reported by Miyakoda and Rosati (1977) in a fine-mesh model.]

Finally, for aspect ratios larger than one, only the non-hydrostatic system is valid. As we have seen in the previous discussion, the hydrostatic system enhances spurious convection and the quasi-hydrostatic system may produce artificially unstable waves (ω^2 changes sign for $k^2/\gamma^2 > 1$). Those results are not surprising since both the hydrostatic and the quasi-hydrostatic systems are far outside the range of validity of the expansion ($\delta < 1$).

In summary then, Fig. 1 divided the aspect ratio axes in three regions:

- Region I: hydrostatic for very small aspect ratios (GCM's with $H/\Delta x \ll 1$).
- Region II: quasi-hydrostatic (mesoscale models for $H/\Delta x \leq 1$).
- Region III: non-hydrostatic (cloud models for $H/\Delta x > 1$).

In the next section let us now examine the comparison of the three systems in a full nonlinear two-dimensional model.

3. Nonlinear two-dimensional integrations

A full nonlinear integration of a two-dimensional atmospheric model using various horizontal resolutions was performed to compare the different approximation methods (hydrostatic, quasi-hydrostatic and non-hydrostatic) with the solutions reported in Orlanski and Ross (1977) and Ross and Orlanski (1978).

a. Description of the model

The numerical model used in the present study is a two-dimensional finite-difference model in which the variables are assumed constant in the y direction. In this particular case for the solution of the circulation and convection of an atmospheric front, the y direction is assumed to be along the axis of the front. The model is 13 km deep; it has the tropopause located at 10 km and a rigid lid at the top ($z = H$). A constant grid (250 m) for the vertical is used for these particular cases. With 76 grid points along the horizontal a constant Δx of 8, 5.33 or 1.33 km was used for the different examples. The model, as described in previous papers, uses open boundary conditions at $x = 0, L$. The prognostic equations are for vorticity (ζ) in the y direction, y momentum (v), potential temperature (θ), relative humidity and liquid water. A streamfunction is calculated from the current vorticity at each time step (τ) as follows:

$$(\alpha_0 \psi_z)_z = \zeta_{(x,z)} \quad \text{hydrostatic} \tag{3.1}$$

or

$$\alpha_0 \frac{\partial^2 \psi}{\partial x^2} + \frac{\partial}{\partial z}\left(\alpha_0 \frac{\partial \psi}{\partial z}\right) = \zeta_{(x,z)} \quad \text{non-hydrostatic,} \tag{3.2}$$

where α_0 is the inverse of the standard density $\rho_0(z)$. The only modification that the quasi-hydrostatic assumption introduces to the hydrostatic calculations from (3.1) is the non-hydrostatic correction

$$\phi_{zz}^{\tau+1} = -\psi_{xx}^{\tau+1} \tag{3.3}$$

and the total quasi-hydrostatic streamfunction is then

$$\psi^{\tau+1} = \psi^{\tau+1} + \phi^{\tau+1} \tag{3.4}$$

b. Moist frontal circulation

The effect of moisture on the dynamics of a mature cold frontal system was investigated by Ross and Orlanski (1978). Lifting produced by the initial cross-stream frontal circulation was shown to have saturated the warm moist air above the nose of the front when the initial humidity levels are sufficiently high. If the atmosphere is convectively unstable, this saturated air will develop into deep convection. The coarse resolution used in this study (20 km) justified the hydrostatic assumption; however, as a test, a comparison was made with the full non-hydrostatic solution (Appendix of Ross and Orlanski, 1978) showing little difference between both solutions.

In this paper we will repeat the calculation for a similar initial condition used in Ross and Orlanski, 1978, namely, a mid-tropospheric jet in geostrophic balance with the potential temperature (Fig. 8, Ross and Orlanski, 1978) advected by a mean synoptic ($\bar{u}$) cross-stream flow. A smaller grid spacing (Δx = 8 km instead of Δx = 20 km) will be used here to enhance the breakdown of the hydrostatic assumption. As mentioned before, the initial conditions were similar to MTJ2 for Ross and Orlanski (1978); since the horizontal scale of the front in this paper is smaller, to preserve a similar shear, the magnitude of V_{MAX} = 15 m s^{-1} was reduced. Hence our purpose is to illustrate the benefits of the newly proposed quasi-hydrostatic approximation and to that end, only realistic examples were considered.

In Fig. 2 the solutions of the hydrostatic, quasi-hydrostatic and non-hydrostatic frontal circulations are shown after 1081 time steps. Y momentum (v component) is shown in the upper part of the figure; streamfunction is shown in the middle and liquid water is shown along the bottom. As we look from left to right we can see that the streamfunction shows an intense cross-stream circulation associated with the convective cloud ahead of the front. At this time of the integration we can clearly see that the streamfunction from the hydrostatic solution has departed drastically from the non-hydrostatic solution. In fact, only 100 time steps later, the hydrostatic solution blows up. On the other hand, the quasi-hydrostatic solution remains quite similar to the non-hydrostatic solution for the length of the integration. In addition, it should be noted that calculations for the non-hydrostatic solution take eight times longer than those of the quasi-hydrostatic solution. We should remember that the quasi-hydrostatic expression is only valid for $H/\Delta x < 1$. If the aspect is larger than 1, internal waves may become weakly unstable. It can be seen that $H/\Delta x$ of the previous example was slightly larger than 1 (13/8). Consequently, the small waves in the upper left of the streamfunction seem to be unstable gravity waves. However, they did not grow more than what is shown in the figure. Those waves excited by the deep convection underneath on the highly stratified region, such as the lower stratosphere, produce these small disturbances which are not completely damped by the low values of the viscosity.

The magnitude of maximum vertical velocity as a function of time for the three cases is shown in Fig. 3. Note that the maximum vertical velocity for the non-hydrostatic and quasi-hydrostatic solutions occurs at the same time but the intensity of the latter is weaker. We also may note that the hydrostatic circulation is weaker than the other two, but it increases to unbounded values soon afterward.

c. Modified quasi-hydrostatic equations (large aspect ratio)

The quasi-hydrostatic system can be easily extended to aspect ratios much larger than 1; how-

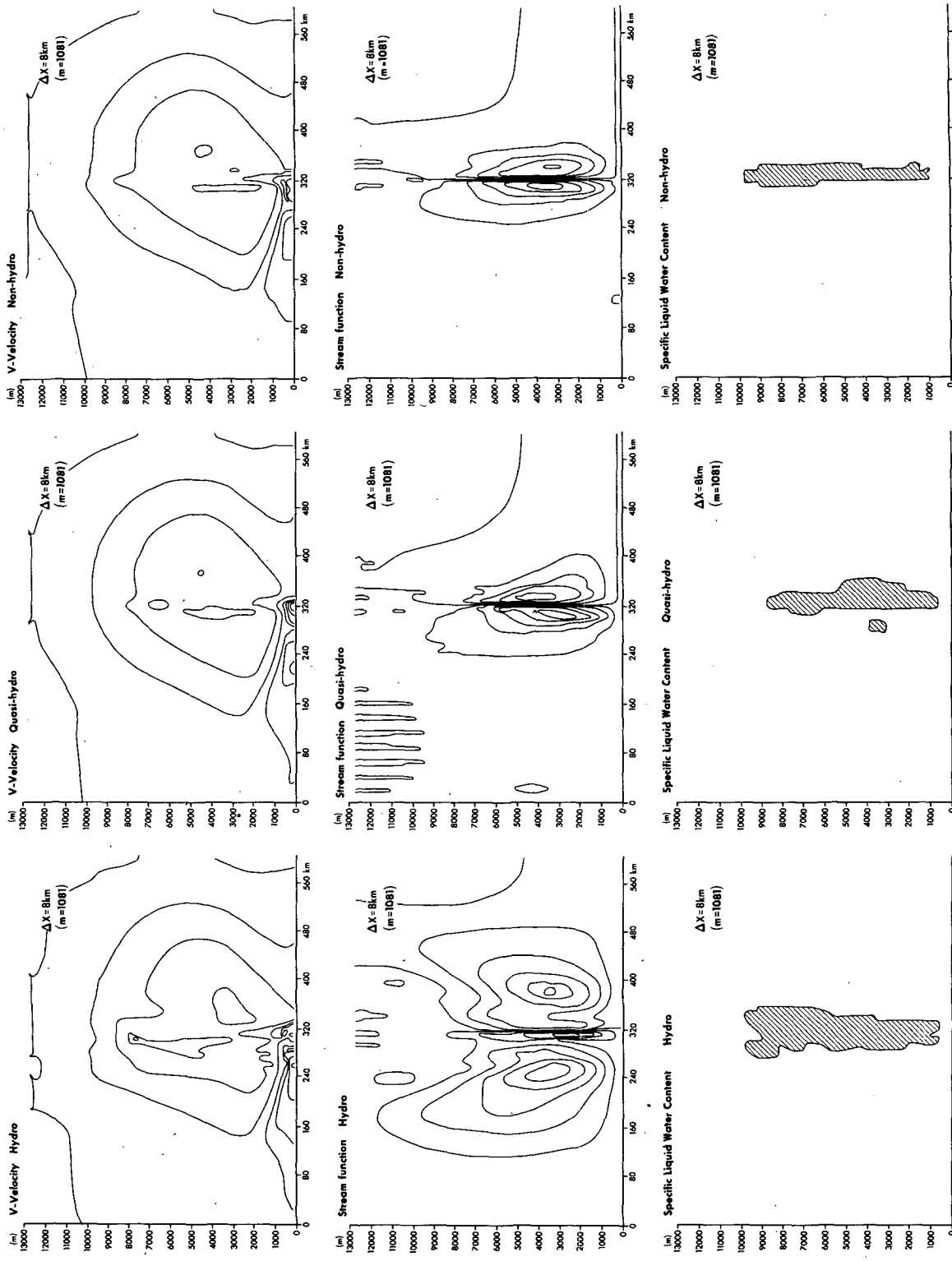

FIG. 2. The composite of a two-dimensional numerical integration of convection associated with a cold front is shown. The V velocity for hydro, quasi-hydro and non-hydrostatic approximations are shown on the upper graphs. The corresponding *streamfunctions* and liquid water for the different approximations are shown in the middle and lower part of the figure.

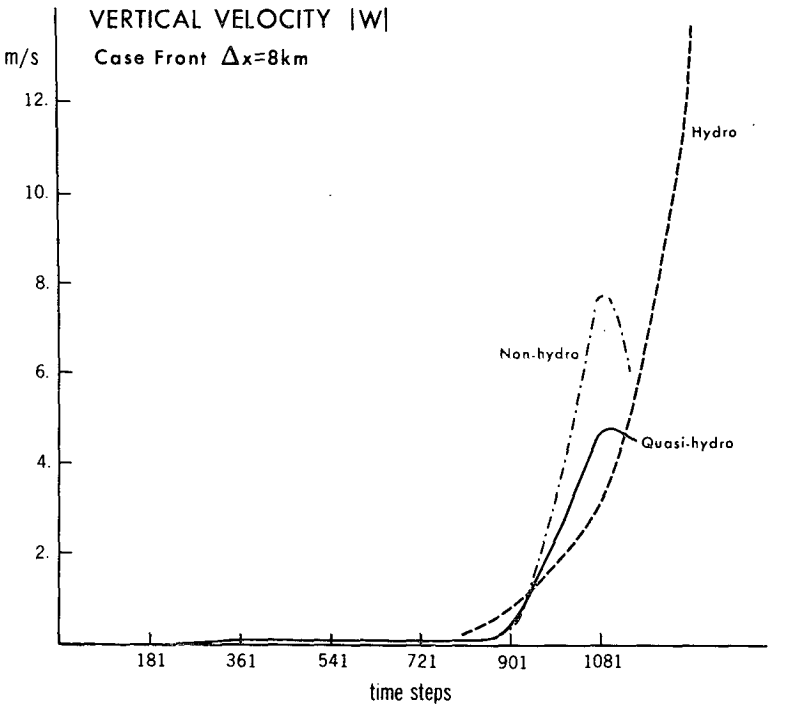

FIG. 3. The amplitude of the maximum vertical velocity as a function of time of integration (in time steps) is shown.

ever, no physical justification can be used for such an extension and one should only view it as a mathematical smoother. Let us briefly examine the testing as shown in (2.6). The non-hydrostatic correction introduces a bi-quadratic term in the dispersion relation and it is this term that goes to zero for aspect ratios of one and which produces unstable gravity for values larger than 1. If the need of the quasi-hydrostatic equation arises for aspect ratios larger than one in the interest of a better numerical simulation for scales close to $H/L \approx 1$, one should remember that $(H/\Delta x)$ determines the aspect ratio that spurious waves may have, whereas H/L with L the order of a few grid points is the aspect ratio of the resolvable dynamics; if these ratios should be close to one, then $H/\Delta x$ must be larger than one with the undesirable feature of unstable gravity waves. It is easy to modify (3.3) to avoid such instability and the procedure is as follows:

$$\phi_{zz}^{\tau+1} = -\beta\psi_{xx}^{\tau+1}. \tag{3.5}$$

The dispersion relation is then given as

$$\omega^2 = \frac{k^2}{\gamma^2} N^2 \left(1 - \frac{\beta^2 k^2}{\gamma^2}\right). \tag{3.6}$$

Now if we prescribe that the disturbance with the highest aspect ratio possible should be stable or neutral, β will be given by $\beta = DX/H$. If the aspect ratio is 1, then the modified quasi-hydrostatic equations are the same as the original set given in (3.3). The coefficient β will not affect the waves that the model can well resolve, only computationally excited waves which may not be of any physical interest will be damped out.

Two examples of convection with different resolutions, $\Delta x = 5.33$ and 1.33 km, are shown in Figs. 4 and 5. The initial conditions are different here than before in that an unstable atmosphere is perturbed by a buoyant bubble which is 1.5°C warmer than its environment. The size of the bubble (6×4) is shown in Fig. 4. The comparison of the modified quasi-hydrostatic and the non-hydrostatic solutions after 1621 time steps is shown in Fig. 5 for the case $\Delta x = 1.33$ km. Note that for these extreme cases, the coefficient CQA for the nonlinear eddy viscosity was increased to 4, thus making them more viscous, but the similarity between both solutions in such severe tests is reasonably good.

4. The three-dimensional quasi-hydrostatic system

A simple extension of the previous results can be applied to derive a consistent three-dimensional set of equations. Since the hydrostatic balance is independent of the compressibility of the fluid, let us then, for simplicity, use the incompressible three-dimensional Boussinesq equations defined as follows:

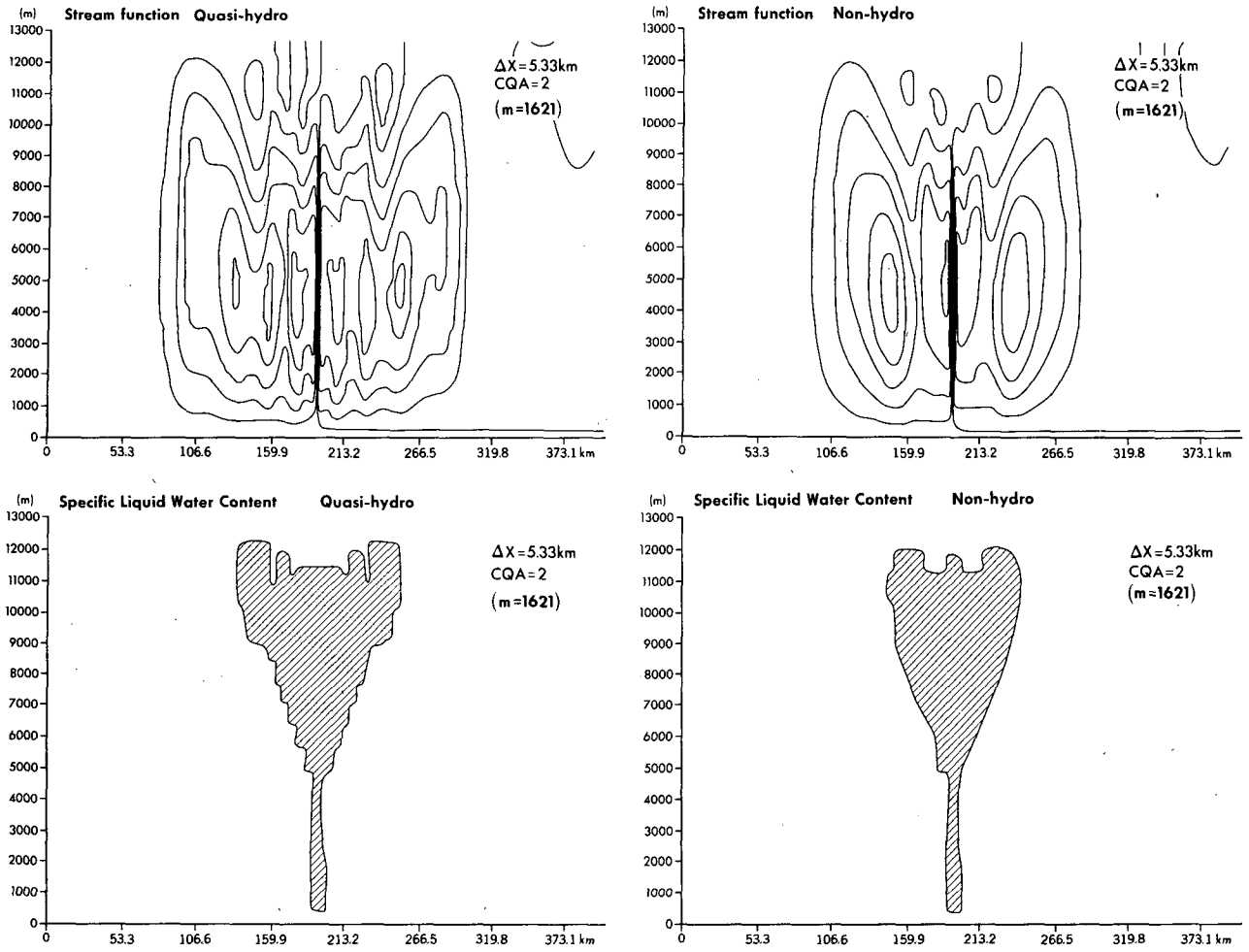

FIG. 4. The simulations of deep convection with an aspect ratio larger than one ($H/\Delta x = 2.264$) for the modified quasi-hydro and the non-hydrostatic approximations are shown.

$$\left.\begin{aligned} \mathbf{V}_t + \mathbf{V}\nabla\mathbf{V} + W\mathbf{V}_z &= -\frac{\nabla p}{\tilde{\rho}} \\ W_t + \mathbf{V}\nabla W + WW_z &= \frac{-Pz}{\tilde{\rho}} + \frac{g\rho'}{\rho} \\ \rho_t + \mathbf{V}\nabla\rho + W\rho_z + W\tilde{\rho}_z &= 0 \\ \nabla\cdot\mathbf{V} + W_z &= 0 \end{aligned}\right\} \quad (4.1)$$

where the equations are perturbations of hydrostatic state at rest [$\bar{P}_z(z) = -g\tilde{\rho}$]. $\mathbf{V}$ is the horizontal vector velocity, W is the vertical component, and p and ρ are the pressure and density, respectively. We can make (4.1) nondimensional by defining the parameters

$$x, y = Lx'y'; \quad z = Hz'; \quad \mathbf{V} = u_r\mathbf{V}'; \quad t = \tau t'$$
$$P = P_rP'; \quad \rho = \rho_r\rho'; \quad w = w_rw'.$$

By substituting and redefining the nondimensional parameters, the Eqs. (4.1) can be written as

$$\left.\begin{aligned} \mathbf{V}_t + \beta\mathbf{V}\nabla\mathbf{V} + \beta W\mathbf{V}_z &= -\hat{p}\beta\nabla p \\ W_t + \beta\mathbf{V}\nabla W + \beta WW_z &= -\frac{\hat{p}\beta}{\delta^2}Pz - N^2\tau^2\rho \\ \nabla\cdot\mathbf{V} + W_z &= 0 \\ \rho_t + \beta\mathbf{V}\nabla\rho + \beta w\rho_z + \beta w\tilde{\rho}_z &= 0 \end{aligned}\right\}, \quad (4.2)$$

where

$$\left.\begin{aligned} &\beta = \frac{\tau u_r}{L} = \frac{\tau w_r}{H} \quad \text{and} \quad \frac{w_r}{u_r} = \delta \\ &\delta = \frac{H}{L}, \quad \hat{P} = \frac{p_r}{\rho_r u_r^2}, \\ &\rho_r = \hat{\rho}\frac{w_r\tau}{g}N^2 \quad \text{and} \quad N^2 = -\frac{gd\tilde{\rho}}{\tilde{\rho}dz} \end{aligned}\right\}.$$

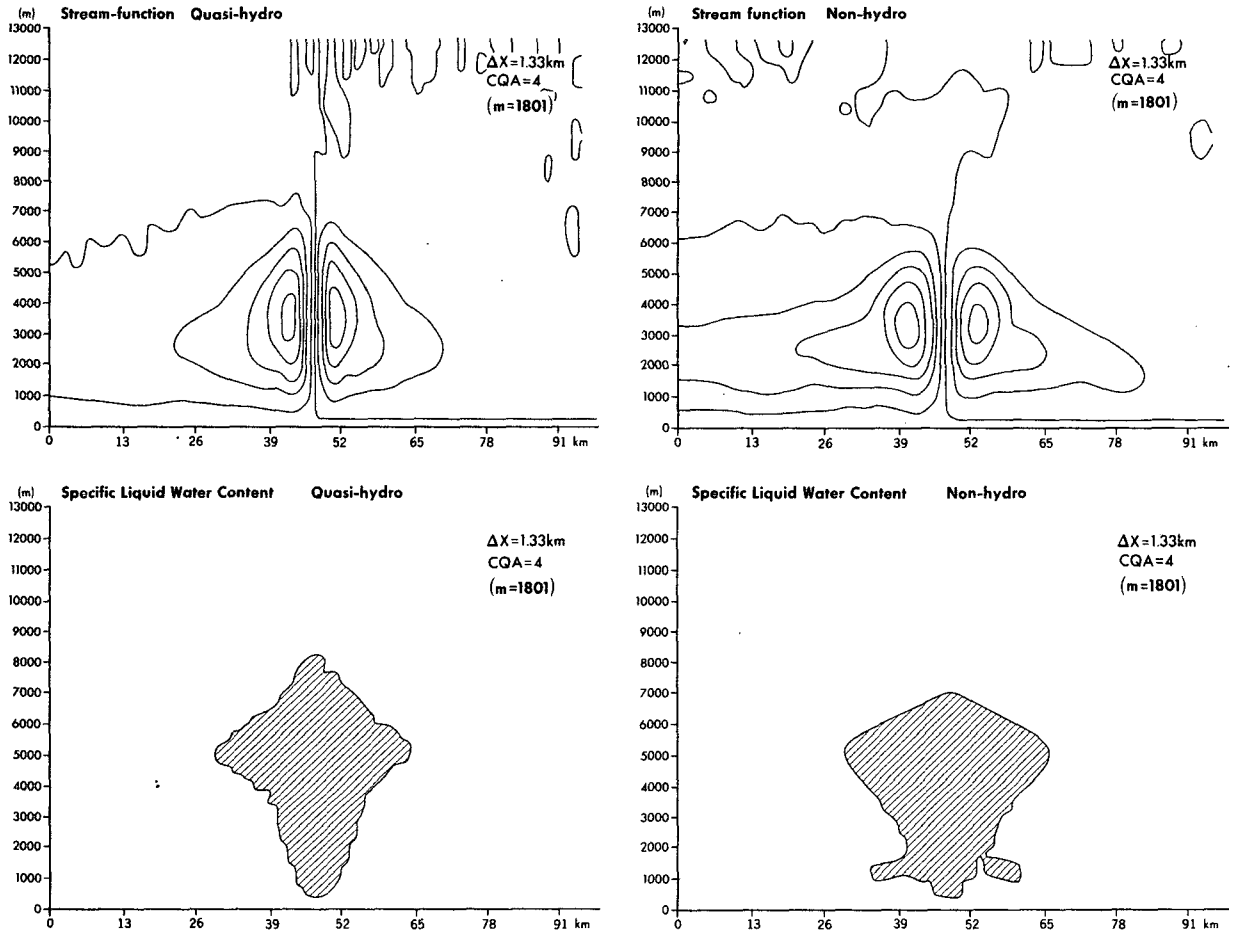

FIG. 5. Extreme example of moist convection with $H/\Delta x = 9$. The streamfunctions are shown in the upper part of the figure; the liquid water content is in the lower portion of the figure.

Note when $\beta \ll 1$ with $\hat{p}\beta \approx O(1)$ and $\beta\tilde{\rho}_z \approx O(1)$, that the system (4.2) becomes a linear set of equations.

$$\left.\begin{aligned} \mathbf{V}_t &= -\nabla p \\ W_t &= -\frac{P_z}{\delta^2} - N^2\tau^2\rho \\ \nabla\cdot\mathbf{V} + W_z &= 0 \\ \rho_t + w\tilde{\rho}_z &= 0 \end{aligned}\right\}. \qquad (4.3)$$

The solution of the form $e^{i\omega t}$ can also be expanded as before:

$$\left.\begin{aligned} \mathbf{V} &= [\mathbf{V}_0 + \delta^2\mathbf{V}_1 + O(\delta^4)]e^{-i\omega t} \\ W &= [w_0 + \delta^2 w_1 + O(\delta^4)]e^{-i\omega t} \\ \rho &= [\rho_0 + \delta^2\rho_1 + O(\delta^4)]e^{-i\omega t} \\ P &= [p_0 + \delta^2 p_1 + O(\delta^4)]e^{-i\omega t} \\ \omega &= \omega_0 + \delta^2\omega_1 + \cdots \end{aligned}\right\}.$$

Notice that ω_0 is of the order of unity because it is nondimensionalized by τ. In fact, for the expansion to be valid, $N^2\tau^2 \approx O(\delta^{-2})$, where $N^2\tau^2 = a\delta^{-2}$ [$a = O(1)$]; this was already shown in Section 2. Substituting in (4.3) and separating by powers of δ^2, we have

$$\delta^0\left\{\begin{aligned} -i\omega_0\mathbf{V}_0 &= -\nabla p_0 \\ P_{0z} &= -a\rho_0 \\ \nabla\cdot\mathbf{V}_0 &= -w_{0z} \\ -i\omega_0\rho_0 + w_0\tilde{\rho}_z &= 0, \end{aligned}\right.$$

and the next order is given as

$$\delta^2\left\{\begin{aligned} -i\omega_0\mathbf{V}_1 - i\omega_1\mathbf{V}_0 &= -\nabla p_1 \\ -i\omega_0 W_0 &= -P_{1z} - a\rho_1 \\ \nabla\cdot\mathbf{V}_1 &= -w_{1z} \\ -i\omega_0\rho_1 - i\omega_1\rho_0 + w_1\tilde{\rho}_z &= 0. \end{aligned}\right.$$

The first-order expansion is the hydrostatic system, whereas the next order correction in δ completes the

quasi-hydrostatic set. In fact, assuming constant coefficients, the zero-order and first-order correction are simple to calculate and are defined as

$$\omega_0 = \pm \frac{k}{\gamma} a,$$

$$\omega_1 = -\omega_0 \frac{k^2}{2\gamma^2}.$$

The dimensional frequency of the second order is then

$$\omega = \pm \frac{k}{\gamma} N\left(1 - \frac{k^2}{2\gamma^2}\right),$$

which is the same as that previously calculated in (3.6). Therefore, what is shown here more clearly than the vorticity treatment of Section 3 is that the quasi-hydrostatic set takes the vertical acceleration from the vertical hydrostatic velocity and generates a correction to the vertical gradient of pressure which modifies the horizontal momentum equation.

This approximation can be applied in a very straightforward manner to finite-difference models or may be included as a modification to existing hydrostatic models.

Finite-difference application

Let us assume that a preexisting set of hydrostatic equations is used and that the prognostic equations at a given time step $\tau + 1$ are defined as follows:

$$\left.\begin{aligned} \mathbf{V}_H^{\tau+1} &= F(\mathbf{V}_T, P_H, \rho_T)^\tau + \mathbf{V}_T^{\tau-1} \\ W_H^{\tau+1} &= \int_0^z \nabla\cdot\mathbf{V}_H^{\tau+1} dz \\ \rho_T^{\tau+1} &= \rho_T^{\tau-1} + G(\mathbf{V}_T, \rho_T)^\tau \\ P_{HZ}^{\tau+1} &= -g\rho_T^{\tau+1} \end{aligned}\right\}.$$

Note that the variables with the subscript H or T refer to being calculated from the hydrostatic pressure (H) or being included in the non-hydrostatic correction (T). To complete the cycle and to evaluate the quasi-hydrostatic contribution for the pressure, we integrate the vertical acceleration from the hydrostatic vertical velocity since $W_H^{\tau+1}$ is known:

$$p_c^\tau(z) = -\int_0^z \frac{dw_H}{dt} dz'.$$

The horizontal velocity correction is then

$$\mathbf{V}_c^{\tau+1} = -\nabla p_c^\tau \cdot Dt$$

and the vertical velocity correction is

$$w_c^{\tau+1} = -\int_0^z \nabla\cdot\mathbf{V}_c^{\tau+1} dz'.$$

Finally, the new set of variables at the current time step are built:

$$\left.\begin{aligned} \mathbf{V}_T^{\tau+1} &= \mathbf{V}_H^{\tau+1} + \mathbf{V}_c^{\tau+1} \\ W_T^{\tau+1} &= W_H^{\tau+1} + W_c^{\tau+1} \end{aligned}\right\}.$$

The density is only a function of velocities at previous time steps and has already been calculated with the corrections included and in this way the cycle is completed.

5. Energy conservation

The three-dimensional Boussinesq equations as defined in (4.1) conserve total energy E [$E = \bar{\rho}(\frac{1}{2}\mathbf{V}^2 + \frac{1}{2}w^2) - \frac{1}{2}g(\rho^2/\bar{\rho}_z)$]. In the hydrostatic limits, however, the energy conservation reduces to conserve the horizontal kinetic plus potential energy only, which is consistent with the assumption that $w^2 \ll \mathbf{V}^2$.

The quasi-hydrostatic system has, as expected, the property of conserving energy to a higher order in the aspect ratio expansion (δ^2) such that, the zero order coincides with the hydrostatic system, whereas non-hydrostatic effects are contained in the higher order. For instance, the vertical kinetic energy is included in the next higher order terms of the expansion.

We now show the form that takes the energy for the quasi-hydrostatic equations by rewriting the nondimensional system defined in (4.2) as

$$\left.\begin{aligned} \frac{d\mathbf{V}}{dt} &= -\hat{P}\beta\nabla p \\ \frac{dw}{dt} &= -(\hat{P}\beta/\delta^2)P_z - N^2\tau^2\rho \\ \frac{d\rho}{dt} &= +w \\ \nabla\cdot\mathbf{V} &= -w_z \end{aligned}\right\}, \qquad (5.1)$$

remembering that the dimensional amplitude for these variables are U_r for $\mathbf{V}$, $w_r = \delta U_r$ for w and $\rho_r = \rho(w_r\tau N^2/g)$ for ρ. We can obtain the equations for the kinetic and potential energies by multiplying the first three equations of (5.1) by V, w and ρ.

$$\left.\begin{aligned} \frac{d\mathbf{V}^2/2}{dt} &= -\hat{P}\beta[\nabla\cdot p\mathbf{V} + (wp)_z] + \hat{P}\beta w p_z \\ \frac{dw^2/2}{dt} &= -\frac{\hat{P}\beta}{\delta^2} wP_z - N^2\tau^2\rho w \\ \frac{d\rho^2/2}{dt} &= +\rho w \end{aligned}\right\}. \qquad (5.2)$$

The system of energy equations in (5.2) is without any approximations; yet, if multiplied by the proper dimensional amplitudes to define the energies, we have

$$\left.\begin{aligned} K_H &= \tilde{\rho} U_r^2 \tfrac{1}{2}\mathbf{V}^2 \\ K_v &= \tilde{\rho} W_r^2 \tfrac{1}{2} w^2 = \tilde{\rho} U_r^2 \delta^2 \tfrac{1}{2} w^2 \\ P^T &= -\frac{g\rho_r^2}{\rho_z} \tfrac{1}{2}\rho^2 = \tilde{\rho} U_r^2 \delta^2 \tau^2 N^2 \tfrac{1}{2}\rho^2 \end{aligned}\right\}. \quad (5.3)$$

The dimensional form of (5.2) is then

$$\left.\begin{aligned} \frac{dK_H}{dt} &= -\hat{P}\beta\tilde{\rho} U_r^2[\nabla\cdot(\mathbf{V}p) + (wp)_z] \\ &\quad + \hat{P}\beta\tilde{\rho} U_r^2(P_z w) \\ \frac{dK_v}{dt} &= -\hat{P}\beta\tilde{\rho} U_r^2(wP_z) - \tilde{\rho} U_r^2\delta^2 N^2\tau^2(\rho w) \\ \frac{dP^T}{dt} &= \tilde{P} U_r^2\delta^2 N^2\tau^2(\rho w) \end{aligned}\right\}. \quad (5.4)$$

Adding the three equations of (5.4) yields

$$\frac{d}{dt}(K_H + K_v + P^T) = -\hat{P}\beta\tilde{\rho} U_r^2[\nabla_0 \mathbf{V} P + (wp)_z]. \quad (5.5)$$

Eq. (5.5) shows the known results that the total energy is conserved. This exercise was done to facilitate the expansion of the energy in powers of δ^2. Using the expansion of the previous section for V, w and P and ρ in the expression of the energy (5.3), it follows that

$$\left.\begin{aligned} K_H &= \tilde{\rho} U_r^2[\tfrac{1}{2}\mathbf{V}_0^2 + \delta^2\mathbf{V}_1\mathbf{V}_0 + O(\delta^4)] \\ K_v &= \tilde{\rho} U_r^2[\delta^2 \tfrac{1}{2} w_0^2 + O(\delta^4)] \\ P^T &= \tilde{\rho} U_r^2 a[\tfrac{1}{2}\rho_0^2 + \delta^2\rho_1\rho_0 + O(\delta^4)] \end{aligned}\right\} \quad (5.6)$$

with the constant $a = N^2\tau^2\delta^2$ in the potential energy previously defined and assumed to be O(1). Therefore, to the zero order the energy conservation takes the form

$$\frac{d}{dt}(\tfrac{1}{2}\mathbf{V}_0^2 + \tfrac{1}{2}a\rho_0^2) = -\hat{P}\beta[\nabla_0(\mathbf{V}_0\rho_0) + (w_0\rho_0)_z],$$

where $\frac{1}{2}\mathbf{V}_0^2 + \frac{1}{2}a\rho_0^2$ is the total energy for the hydrostatic system. The expansion (5.6) can be applied to each term in (5.4) obtaining in order of δ^2 the contributions of the quasi-hydrostatic approximation:

$$\mathrm{O}(1)\left\{\begin{aligned} \frac{dK_{H0}}{dt} &= \frac{d}{dt}\frac{(\mathbf{V}_0^2)}{2} \\ &= -\hat{P}\beta[\nabla\cdot\mathbf{V}_0 P_0 + (w_0 P_0)_z] \\ &\quad + \hat{P}\beta W_0 P_{0z} \\ 0 &= -\hat{P}\beta w_0 P_{0z} - a(\rho_0 w_0) \\ \frac{dP_0^T}{dt} &= \frac{d(a\rho_0^2)/2}{dt} = a\rho_0 w_0 \end{aligned}\right. \quad (5.7)$$

and

$$\mathrm{O}(\delta^2)\left\{\begin{aligned} \frac{dK_{H1}}{dt} &= \frac{d(\mathbf{V}_1\mathbf{V}_0)}{dt} \\ &= -\hat{P}\beta[\nabla\cdot(\mathbf{V}_1 P_0 + \mathbf{V}_0 P_1) \\ &\quad + (w_1 P_0)_z + (w_0 P_1)_z] \\ &\quad + \hat{P}\beta(w_1 P_{0z} + w_0 P_{1z}) \\ \frac{dK_{v1}}{dt} &= \frac{d(w_0^2)/2}{dt} \\ &= -(\hat{P}\beta w_1 P_{0z} + a w_1\rho_0) \\ &\quad - (\hat{P}\beta w_0 P_{1z} + w_0\rho_1) \\ \frac{dP_1^T}{dt} &= \frac{ad(\rho_1\rho_0)}{dt} = a(\rho_1 w_0 + \rho_0 w_1). \end{aligned}\right. \quad (5.8)$$

The energy system (5.7) shows, as stated before, the conservation of energy in the hydrostatic approximation. Note that, instead of the vertical kinetic energy equation, the hydrostatic balance is shown in the second equation of (5.7).

The non-hydrostatic contributions are shown in (5.8) where the first and third equations are the modifications of the horizontal kinetic and potential energies, respectively. The second equation now represents the time derivative of the vertical kinetic energy. Notice that terms containing w_1 in this equation cancel by the hydrostatic balance ($w_1 P_{0z} = -w_1\rho_0$) giving a direct transfer of potential to horizontal kinetic energy by these terms. The second term on the right-hand side of the second equation determines to this order the energy transfer form vertical to horizontal kinetic energy ($w_0 P_{1z}$) and $a(w_0\rho_1)$ the transfer from vertical kinetic to potential energies, thus proving that, $E_1 = \mathbf{V}_1\mathbf{V}_0 + w_0^2/2 + a\rho_1\rho_0$ is conserved. Regrouping terms, the total energy conserved for the quasi-hydrostatic system is then

$$E_q = \tilde{\rho} U_r^2[\tfrac{1}{2}\mathbf{V}_0^2 + \tfrac{1}{2}a\rho_0^2 + \delta^2(\mathbf{V}_0\mathbf{V}_1 + \tfrac{1}{2}w_0^2 + a\rho_0\rho_1)].$$

6. Conclusions

Mesoscale modeling requires scales with aspect ratios close to 1, for such models the validity of the hydrostatic assumption cannot be assured, particularly, when deep convective systems are studied, leaving only the option of considering more complicated and often more expensive non-hydrostatic systems. In this paper a practical approach to encompass the limitations of the hydrostatic models is presented.

The expansion in powers of the aspect ratio ($\delta = H/L$) for the full three-dimensional equations of motion suggests a slight modification to the hydrostatic system that retains non-hydrostatic

properties and considerably improves the simulation of mesoscale dynamics.

A comparison of two-dimensional numerical simulations with the hydrostatic, quasi-hydrostatic, and non-hydrostatic equations for deep convection in a frontal system shows a clear improvement of the new suggested scheme as compared with the hydrostatic one. The solutions of the quasi-hydrostatic and non-hydrostatic equations are very similar in three experiments shown in this paper, which were the dynamics of an atmospheric front, and two free-convection experiments with aspect ratios larger than one.

The experiments were not intended to be realistic, in fact they were found to be more vigorous than those observed in nature to illustrate the differences, if any, between the quasi-hydrostatic and non-hydrostatic systems.

The quasi-hydrostatic system is slightly less economical than the hydrostatic one, but still more economical than the non-hydrostatic calculations. In fact, the two-dimensional calculations shown, are found to be eight times faster than the full non-hydrostatic calculations. A drawback of this new scheme appears to be that gravity waves with aspect ratios larger than one are unstable; however, this may not be significant since the whole expansion should not apply to aspect ratios larger than 1.

Finally, a new form of energy consistent with the quasi-hydrostatic approximation is shown to be conserved.

Acknowledgments. The author is very grateful to Professor Y. Ogura for suggesting the energy consideration, and to Dr. K. Miyakoda, Dr. B. Ross and Mr. L. Polinsky for reading the manuscript. The author also extends his appreciation to Betty Williams for typing the manuscript, and to the GFDL drafting group for preparing the figures.

REFERENCES

Miyakoda, K., and T. Rosati, 1977: One-way nested grid models: The interface conditions and the numerical accuracy. *Mon. Wea. Rev.*, **105**, 1092–1107.

Orlanski, I., and B. B. Ross, 1977: The circulation associated with a cold front. Part I: Dry case. *J. Atmos. Sci.*, **34**, 1619–1633.

Ross, B. B., and I. Orlanski, 1978: The circulation associated with a cold front. Part II: Moist case. *J. Atmos. Sci.*, **35**, 445–465.